International Journal of Biometeorology (2023) 67:93–105
https://doi.org/10.1007/s00484-022-02388-x

ORIGINAL PAPER

Malaria metrics distribution under global warming: assessment of the VECTRI malaria model over Cameroon

Amelie D. Mbouna[1] · Alain T. Tamoffo[1,2] · Ernest O. Asare[3] · Andre Lenouo[4] · Clement Tchawoua[1]

Received: 20 January 2022 / Revised: 30 June 2022 / Accepted: 11 October 2022 / Published online: 18 October 2022

Abstract

Malaria is a critical health issue across the world and especially in Africa. Studies based on dynamical models helped to understand inter-linkages between this illness and climate. In this study, we evaluated the ability of the VECTRI community vector malaria model to simulate the spread of malaria in Cameroon using rainfall and temperature data from FEWS-ARC2 and ERA-interim, respectively. In addition, we simulated the model using five results of the dynamical downscaling of the regional climate model RCA4 within two time frames named near future (2035–2065) and far future (2071–2100), aiming to explore the potential effects of global warming on the malaria propagation over Cameroon. The evaluated metrics include the risk maps of the entomological inoculation rate (EIR) and the parasite ratio (PR). During the historical period (1985–2005), the model satisfactorily reproduces the observed PR and EIR. Results of projections reveal that under global warming, heterogeneous changes feature the study area, with localized increases or decreases in PR and EIR. As the level of radiative forcing increases (from 2.6 to 8.5 $W.m^{-2}$), the magnitude of change in PR and EIR also gradually intensifies. The occurrence of transmission peaks is projected in the temperature range of 26–28 °C. Moreover, PR and EIR vary depending on the three agro-climatic regions of the study area. VECTRI still needs to integrate other aspects of disease transmission, such as population mobility and intervention strategies, in order to be more relevant to support actions of decision-makers and policy makers.

Keywords PR · EIR · Global warming · RCA4 · VECTRI

Introduction

The World Health Organization (WHO report 2015) reports that malaria remains one of the most important killer diseases in the world. Eighty-two percent of the cases and 94% of deaths are recorded in Africa. Malaria, therefore, is the primary cause of mortality and morbidity in Africa (WHO report 2008). This disease is endemic in tropical and subtropical areas, and sub-Saharan African countries continue to be the most affected. Specifically in Cameroon, the illness is the leading cause of mortality and morbidity with children under five and pregnant women being the most affected (Bandolo 2012). In 2006, there were approximately 5 million cases of malaria in the country (WHO report 2008), making the disease the country's priority health issue.

Malaria is caused by a parasite which is a protozoan from the genus plasmodium and transmitted to people through the bites of infected female mosquitoes. A single bite by a malaria-carrying mosquito can lead to extreme sickness or death. Malaria starts with extreme cold, followed by a high fever and severe sweating. These can be accompanied by joint pain, abdominal pain, headaches, vomiting and extreme tiredness.

Malaria disease is very sensitive to climatic conditions, and in tropical areas, the disease is prevalent (Bomblies and Eltahir 2009), because of the abundance of mosquitoes' breeding sites and favourable weather conditions. The

✉ Amelie D. Mbouna
ameldany18@gmail.com

1 Laboratory for Environmental Modelling and Atmospheric Physics (LEMAP), Department of Physics, Faculty of Science, University of Yaoundé I, P.O. Box 812, Yaounde, Cameroon

2 Physics Department, Kwame Nkrumah University of Science and Technology, Kumasi, Ghana

3 Department of Epidemiology of Microbial Diseases, Yale School of Public Health, Yale University, New Haven, USA

4 Department of Physics, Faculty of Science, University of Douala, Douala, Cameroon

link between climate and malaria is well documented. In fact, rainfall and temperature influence the life cycles of the anopheles' mosquito vector as well as the malarial parasite *plasmodium falciparum* (Lindsay et al. 2000; Abiodun et al. 2018). Temperature determines the length of the mosquito cycle and the sporogonic cycle of the malarial parasite within the mosquito (Hajison et al., 2017; Egbendewe-Mondzozo et al. 2011). Rainfall provides suitable temporary water bodies (breeding sites) for mosquitoes to grow and develop (Komen et al 2015; Garske et al. 2013). But extreme rainfall appears to be harmful to mosquito development, as it flushes out mosquitoes from their aquatic habitat and kills them (Paaijmans et al., 2007).

The disease sensitivity to climate can also be demonstrated using models. In fact, considerable efforts are made by scientists by constructing some mathematical models to forecast malaria distribution. For instance, Ayanlade et al. (2020) demonstrated the modulator effect of rainfall and temperature indices on malaria propagation with a high Spearman correlation coefficient for rainfall as well as temperature. Ermert et al. (2012) using the Liverpool malaria model (LMM) demonstrated the strong influence of changes in rainfall and temperature on the malaria distribution in various ecological African zones. Diouf et al. (2017) also established with the LMM that the risk of malaria transmission is mainly associated with variability in rainfall and temperature.

Among studies related to climate change and malaria, Ye et al. (2007) found that rainfall and temperature significantly influence the malaria's incidence with emphasis on temperature. In some West African countries, Diouf et al. (2020) demonstrated that the malaria's high transmission periods are directly linked to heavy rainfall events. Malaria endemicity would be little affected by climate change (Beguin et al. 2011). This suggests that warm temperatures (due to global warming) are likely to increase or/and decrease malaria in endemic areas. In fact, high temperatures could significantly impact growing conditions of the mosquito. However, the temperature might not be the only factor as the WHO's report in 1975 highlighted the migration's effect of population from endemic zones to free malaria areas on the dynamics of the malaria disease. This aspect is supported by previous work by Ngarakana-Gwasira et al. (2016). In addition, the impact of global warming on the health is not expected to be homogenous across regions as Costello et al. (2009) argued.

Numerous studies across Africa (e.g. Peterson 2009, Yamana et al. 2016) project a gradual southward shift of malaria from the Sahelian zones of the West African, including northern Cameroon. This may suggest unfavourable conditions for malaria proliferation by the 2080s (Caminade et al. 2014). Other studies demonstrated inconsistencies between projected changes in malaria spread and global warming, especially over the Sahel (Beguin et al. 2011; Escobar et al. 2016).

A study conducted by Asare and Amekudzi (2017) using the Abdus Salam International Centre for Theoretical physics (ICTP) vector borne disease model (VECTRI) also simulated malaria transmission dynamics at both national and local scales in Ghana and specified the predominant role of rainfall. Mbouna et al. (2019) modelled the malaria distribution over Cameroon using the VECTRI malaria model. They showed that malaria prevalence is maximum at temperatures of 24 to 26 °C and rainfall rates of approximately 4 to 6 mm/day. This rainfall amount features a smaller rate in locations far from water bodies and where the transmission seasonality is close to that of rainfall with a lag of 1 to 2 months (also found by Diouf et al. 2020), satisfactorily simulated by the VECTRI model. The particularity of the VECTRI model is that apart from temperature and rainfall, it pays particular attention to the human population density's modulator effect on the malaria transmission and distribution (Caminade et al. 2014).

Although several studies demonstrated the performances of VECTRI coupled with temperature and rainfall to simulate malaria metrics, studies conducted under global warming are still needed. Yet, such analyses might contribute to a long-term plan for disease prevention, adaptation and mitigation of the transmission. Therefore in the present study, we use the VECTRI model with the atmospheric regional climate model RCA4 (VECTRI-RCA4) to address the issue. The goal of the study is twofold: first, assess the ability of the combination VECTRI-RCA4 to model malaria metrics over Cameroon and, second, explore the impact of global warming under the Representative Concentration Pathway (RCP) 2.6 and 8.5 on malaria distribution. Through examination of projections, we hope to portray preliminary aspects of malaria propagation in a warmer world over Cameroon, as well as alerting decision-makers to the challenges and opportunities for mitigation. The paper is organized as follows: the "Data and methods" section describes the data and methods used. The "Results and discussion" section presents the obtained results and discusses the key findings. A summary concludes this work in the "Conclusion" section.

Data and methods

Study area

Our study domain is Cameroon, located over Central Africa within latitudes 1.5°N–13°N and longitudes 8°E–17°E, an area covering other neighbouring countries as presented in Fig. 1.

Cameroon's climate varies from humid in the south to arid and hot in the north. Cameroon's climate is particularly

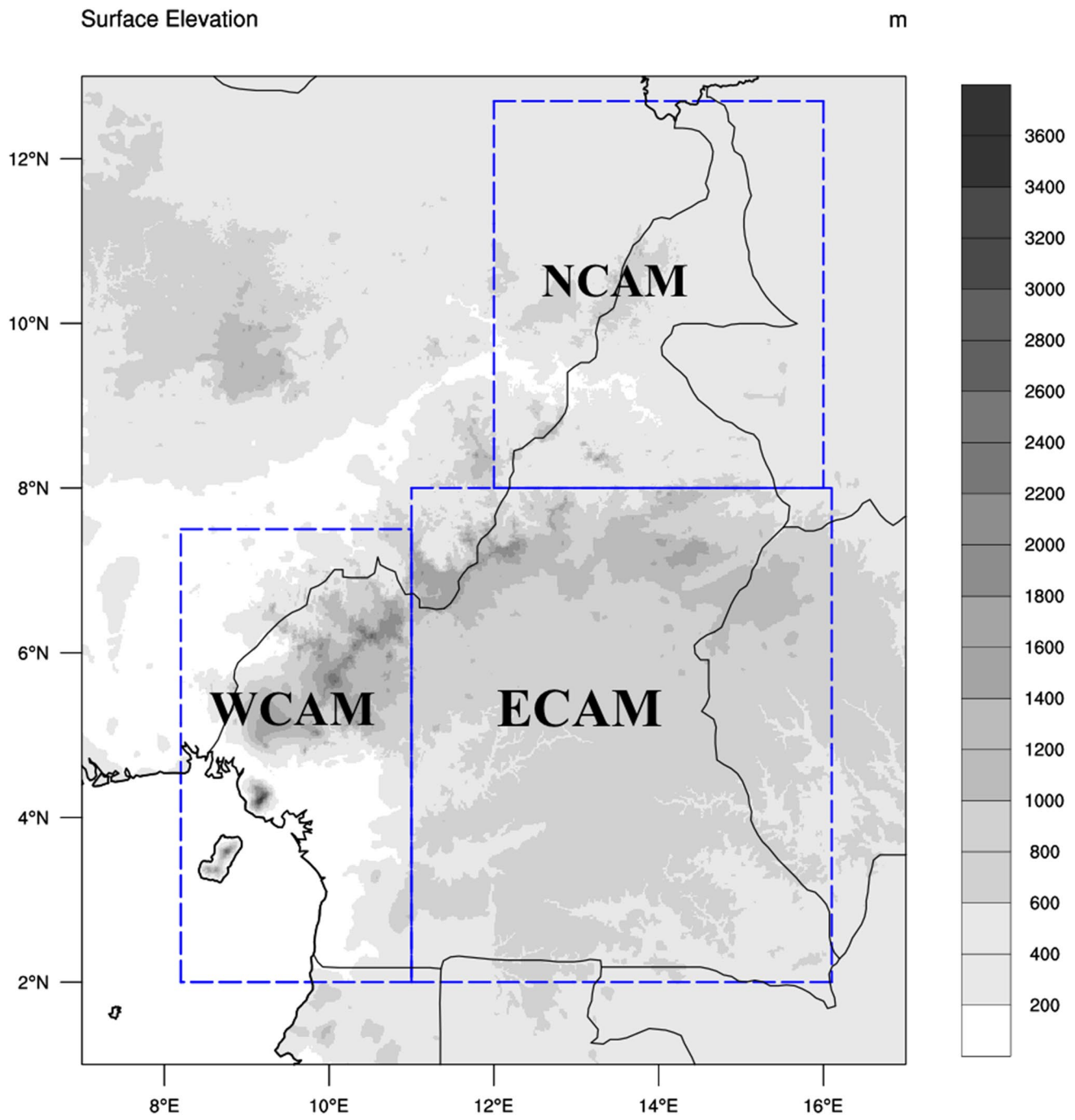

Fig. 1 Map of Cameroon and neighbouring countries. Highlighted in blue are the three agro-climatic sub-regions: North Cameroon (NCAM), West Cameroon (WCAM) and East Cameroon (ECAM)

influenced by the Harmattan and the Atlantic Monsoon winds and is then characterized by two climatic domains, namely the tropical and the equatorial domain (Zaroug and Reynolds 2006; Molua and Lambi 2007). The area has also been subdivided into three agro-climatic sub-regions, namely the North Cameroon (NCAM), West Cameroon (WCAM) and East Cameroon (ECAM).

VECTRI malaria model

The model used in this work is an open-source, the Abdus Salam International Centre for Theoretical Physics (ICTP) vector borne disease model (VECTRI). VECTRI is a grid distributed dynamical model that couples a biological model for the vector and parasite life cycles, to a simple

compartmental Susceptible-Exposed-Infectious-Recovered (SEIR) representation of the disease progression in the human host. VECTRI has the particularity to incorporate interactions between the human host (H) and vectors using the human biting rate (hbr) expressed as presented in Eq. 1 as follows (Tompkins and Ermert 2013).

$$hbr = \left(1 - e^{\frac{-H}{\tau zoo}}\right) \frac{\sum_{j=1}^{N_{sporo}} V(1,j)}{H} \quad (1)$$

The factor 1-exp(-H/τ_{z00}) represents the level of vector zoophily. The exponential factor reflects this, with the e-folding population density for the effect set to $\tau zoo = 50\ \mathrm{km}^{-2}$. The vector status is also bin resolved, consisting of two properties: the gonotrophic and sporogonic cycles. It is thus represented as a two dimensional array $V(Ngono, Nsporo)$. All vectors in the first gonotrophic bin $\sum_{j=1}^{Nsporo} V(1,j)$ are in the meal-searching step of the model.

The probability of transmission of an infectious vector to the host after a single bite is noted as P_{vh}. If its value is assumed constant, then the probability of transmission for an individual receiving n infection bites is given by $1-(1-P_{vh})^n$. The daily overall transmission probability per person is then expressed as in Eq. 2 (Tompkins and Ermert 2013):

$$P_{v\to h} = \sum_{n=1}^{\infty} G_{\overline{EIR_d}}(n)\left(1 - \left(1 - P_{vh}\right)^n\right) \quad (2)$$

G_{EIR} is the Poisson distribution for mean entomological inoculation rate (EIR). EIR, which is the daily number of infectious bites by infectious vectors, is calculated as the product of human biting rate (hbr) and circumsporozoite protein rate (CSPR). Equation 2 is subject to modification if factors such as the use of mosquito nets, which cause fluctuations in the biting rate, are to be taken into account. Generally, a population host has about 20 days after infection to assume the infective status (Day et al. 1998). The calculation of parasite ratio (PR) and EIR relies on both Eqs. 1 and 2 of the VECTRI model. Further information on the physical and mathematical formulation is available in the supplementary material.

Data used

Climate inputs for VECTRI, specifically rainfall and temperature data at 0.44° grid spacing,are taken from the results of dynamical downscaling of the fourth version of the Rossby Centre Atmospheric (RCA) model (RCA4), participating in the Coordinated Regional Climate Downscaling Experiment (CORDEX) project. RCA4 was forced with five global climate models (GCMs) involved in the Coupled Model Intercomparison Project phase 5 (CMIP5; Taylor et al. 2012). Details of downscaled GCMs are provided in Table 1.

Observed malaria PR data are obtained from the Malaria Atlas Project programme (MAP) that collects results of individuals researchers or organizers already published in the literature while EIR is obtained from a recent database for Africa (Yamba et al. 2020).

VECTRI was first integrated from January 1985 through December 2005 using historical data from the downscaled GCMs which is compared against simulations when VECTRI is forced by the observation FEWS-ARC2, Famine Early Warning Systems Network ARC version 2 (Love 2002) for rainfall and the reanalysis ECMWF ERA-Interim (Dee et al. 2011) for temperature. Secondly, the model is integrated under global warming using two Representative Concentration Pathway scenarios: the high-mitigated, low-emission RCP2.6 and the low-mitigated, high-emission RCP8.5 scenarios (Vuuren et al. 2011). Using these two contrasted scenarios enables us to get an insight into the way each warming level might impact the malaria metrics' distribution over Cameroon. Therefore, this offers the possibility to stimulate discussion about the opportunity or not to mitigate the changing climate.

Population density is taken from AFRIPOP (Linard et al. 2012) for each grid cell point in order to account for the growth of the population in the malaria simulations. We set the population growth parameter in VECTRI to be equal to the annual population growth rate in Cameroon, which is 2.6 according to the results of the third National Population Census (Mbarga 2010) taking advantage of the fact that the model is dynamic. VECTRI's simulations are performed with a $0.1° \times 0.1°$ horizontal resolution. Driving data are statistically downscaled to the land model

Table 1 Details of GCMs used to force RCA4 in this study

Model name	Institution	Native resolution	References
EC-EARTH-ES	European community Earth-System Model Consortium	1.125◦ × 1.125◦	Hazeleger et al. (2010)
MPI-ESM-LR	Max Planck Institute for Meteorology	1.9◦ × 1.9◦	Popke et al. (2013)
MIROC-5	Atmosphere and Ocean Research Institute (University of Tokyo)	1.40◦ × 1.40◦	Watanabe et al. (2011)
NorESM1-M	Norwegian Climate Centre	2.5◦ × 1.9◦	Bentsen et al. (2013)
HadGEM2-ES	Met Office Hadley Centre	1.875◦ × 1.25◦	Collins et al. (2011)

resolution assuming a lapse rate of 6.5 K km^{-1} to adjust to the high-resolution topography.

Results and discussion

Models' evaluation

This section aims at evaluating the ability of the RCA4 model to reproduce the climatology of the study area as well as the VECTRI model to simulate malaria (malaria metrics) observed data.

RCA4 model evaluation

We started by investigating whether the atmospheric regional climate model RCA4 satisfactorily reproduces the mean climatology of Cameroon rainfall and temperature. To this, we investigated the three agro-climatic sub-regions termed North Cameroon (NCAM), West Cameroon (WCAM) and East Cameroon (ECAM) (see Fig. 1). Only the results based on the ensemble mean of RCM experiments (RCA-EnsMean thereafter) are presented in the main document, whereas outcomes from individual RCM simulations are shown in the supplementary material.

Figure 2 shows the seasonality of rainfall (left panels) and temperature (right panels) over the three agro-climatic regions. The grey shade band is the standard deviation

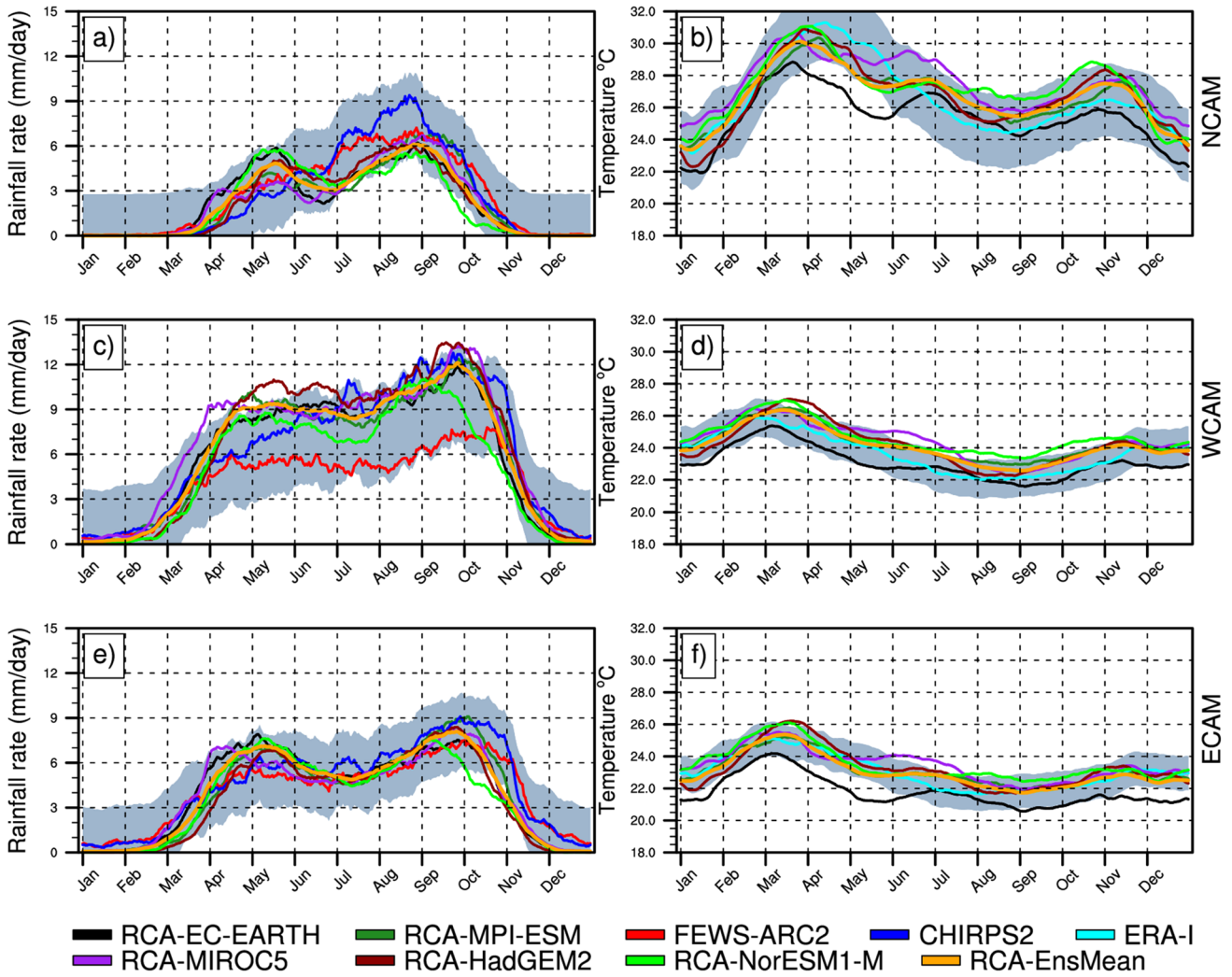

Fig. 2 Seasonality of mean (1985–2005) rainfall (in mm/day, left panels) and temperature (in °C, right panels). The study area is subdivided into three agro-climatic regions: **a**, **b** North Cameroon (NCAM, row 1), **c**, **d** West Cameroon (WCAM, row 2) and **e**, **f** East Cameroon (ECAM, row 3). Data used are from RCA4 simulations and the ensemble mean of RCM runs (RCA-EnsMean) and from observed rainfall FEWS-ARC2 (red), CHIRPS2 (blue). The temperature reference is extracted from the ERA-Interim (cyan) reanalysis dataset

obtained from the FEWS-ARC2 for precipitation and from the reanalysis ERA-Interim for the temperature. For a given month, a mean rainfall value greater than the corresponding standard deviation is considered as a clear failing of the considered experiment. Two peaks are observed for rainfall in WCAM (Fig. 2a) and ECAM (Fig. 2e) in May and October (highest peak at ~12 mm/day and ~9 mm/day respectively), while NCAM experiences a unimodal rainfall regime, with the peak (~9 mm/day) occurring during August to September months (Fig. 2c). Although some divergences in terms of rainfall magnitude are noticed between datasets (more pronounced in NCAM), they all nevertheless vary within the range of the observed standard deviation. The seasonality of temperature is also well captured with the highest values in March and the ones in December for WCAM (Fig. 2b) and ECAM (Fig. 2f). Two obvious peaks are observed within April to May (up to 30 °C) and within November to December (up to 28 °C) for NCAM (Fig. 2d). RCA-EC-EARTH failed to simulate the temperature for NCAM from April to June (Fig. 2d); from April to June and from November to December over ECAM (Fig. 2f). Overall, the climatological annual cycle of both rainfall and temperature are realistically captured over all subregions. The RCA-EnsMean is quite similar to individual RCM runs and is well contained in the natural variability of observations. This suggests that the ensemble mean of experiments is representative of individual simulations and can be used without changing the conclusion.

Statistical performance measures are summarized in Fig. 3, through the Taylor diagram. Three statistical metrics are used, including the root-mean-square difference (RMSD), the pattern correlation (r) and the standard

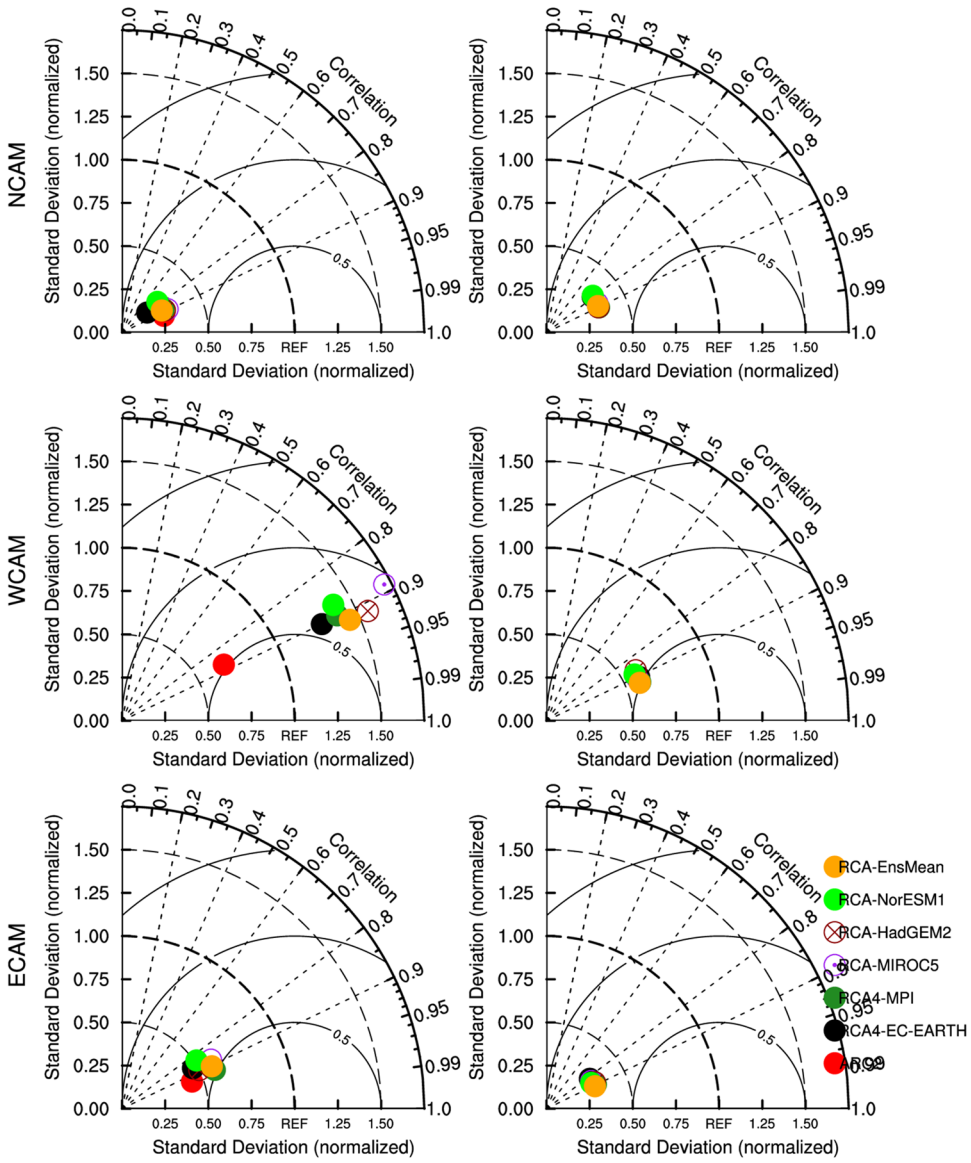

Fig. 3 Taylor diagrams displaying the statistics of daily precipitation and comparing RCA4's experiments and the ensemble mean (RCA-EnsMean) with observations FEWS-ARC2 (reference field for precipitation). For temperature, the reanalysis ERA-Interim is used as a point of reference. The first row shows statistical parameters over NCAM, the second over WCAM and the third over ECAM. The first column displays statistical parameters for precipitation while the second does so for temperature

deviation (STD), computed between downscaled results and FEWS-ARC2 for precipitation, and ERA-Interim for temperature used as a point of reference.

Regarding precipitation statistics, for NCAM and ECAM, RCA4's experiments and FEWS-ARC2 clustered but not so close to the reference field with average performances (RMSD < 1; r ~ 0.90 and STD < 0.75). There are fewer performances of RCA4's model for WCAM compared to the reference field with 1 < RMSD < 1.5, r ~ 0.90 and 1 < STD < 1.5. For temperature, RCA4's runs clustered and outperformed (compared to what was observed with precipitation) over the three agro-climatic regions, with r ~ 0.90, 0.5 < RMSD < 1 and STD < 0.75.

VECTRI model evaluation

Figure 4 presents how observed PR and EIR (blue lines) fit with simulated values (red lines) over the different measurement stations. Here, simulated values are results of the combination VECTRI-RCA-EnsMean, i.e. VECTRI driven by RCA-EnsMean. The PR and EIR observed and simulated values in Fig. 4 can be found in Table S1 and Table S2 in the supplementary material.

The results show that, although there are differences between the two experiments, the shapes of the curves are similar, meaning that the combination VECTRI-RCA-EnsMean succeeds to detect the signal of individual stations. The differences can be attributed to differences in rainfall amount and temperature. VECTRI outperforms in simulating EIR (right panel) than PR (left panel). It is important to recall the challenge of assessing model performance over equatorial Africa given observational uncertainty. Some differences may be associated with inhomogeneities in station measurements. The fact that the combination VECTRI-RCA-EnsMean satisfactorily reproduces the signal of variation of PR and EIR in most stations makes its usage reliable for projection.

To get an insight into how the coupling VECTRI-RCA-EnsMean simulates the spreading of malaria over the country, we showed in Fig. 5 the spatial distribution of the PR as modelled by VECTRI-RCA-EnsMean compared against the monthly observed PR over the period 1985–2005.

These spatial plots present a varied landscape of malaria PR over the country. There are some simulated biases in NCAM where PR values are above 0.5 (Fig. 5b) which is mostly dry and warm, whereas in the observation (Fig. 5a), the mean PR is lower. Such a difference could be probably related to the sensitivity of VECTRI to low rainfall. For ECAM, the differences in PR between observed and simulated values are more obvious compared to WCAM. The model somehow outperforms better in these two areas compared to the NCAM.

Projected changes in the malaria metrics

In this section, we explore the impacts of global warming on the aforementioned malaria metrics under the optimistic (RCP2.6) and the pessimistic (RCP8.5) scenarios. Analyses are conducted under two-time frames: the near future (2035–2065) and the far future (2071–2100), using the combination VECTRI-RCA-EnsMean.

Changes in the parasite ratio (PR)

Figures 6 and 7 exhibit the monthly mean changes in PR over the near future and the far future under the high mitigated RCP2.6 (Fig. 6) and the low mitigated RCP8.5 (Fig. 7) scenarios.

Figure 6 presents the PR pattern obtained with RCA-EnsMean, under RCP2.6 scenario. Results based on individual experiments are presented in the supplementary material as follows: Fig. S1 for RCA4-EC-EARTH-ES, Fig. S3 for RCA4-MPI-ESM-LR, Fig. S5 for RCA4-MIROC5, Fig. S7 for RCA4-HadGEM2 and Fig. S9 for RCA4-NorESM1-M.

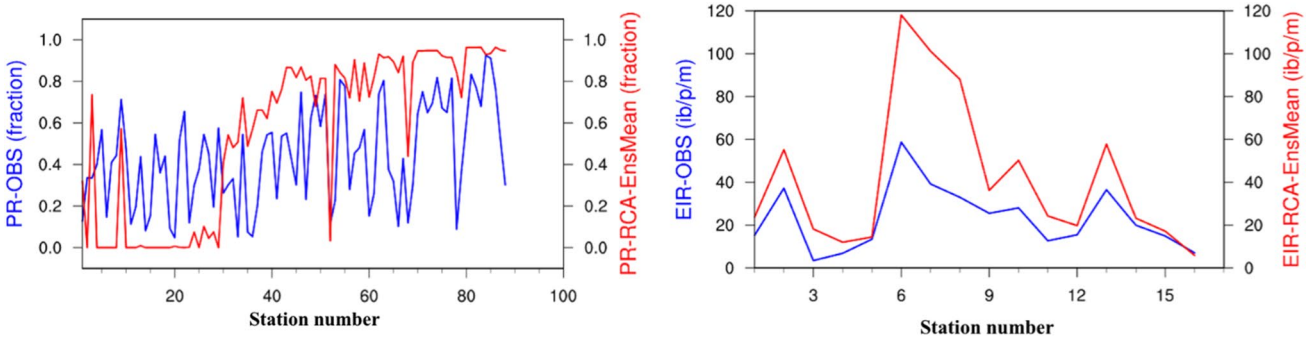

Fig. 4 Results of combinations of VECTRI-observation (in blue) and VECTRI-RCA-EnsMean (in red) for PR (left panel) and EIR (right panel), function of rainfall (mm/day) and temperature (°C) over Cameroon. The x-axis values represent the station number. The two panels show how VECTRI forced with observed station measurements compares against VECTRI forced with RCA-EnsMean

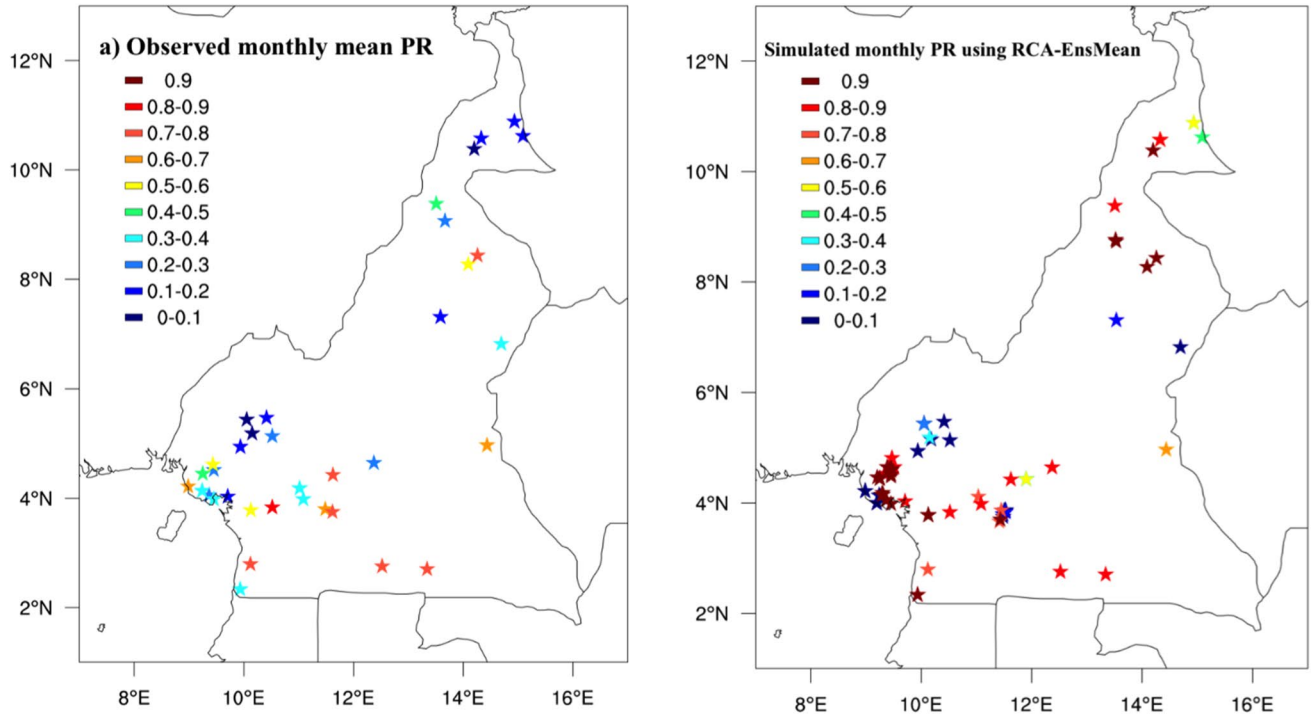

Fig. 5 Observed (left) and simulated (right) monthly mean of PR for the available data sites in Cameroon over the period 1985–2005. The PR values represent the average of all the points located within the same geographical areas of study

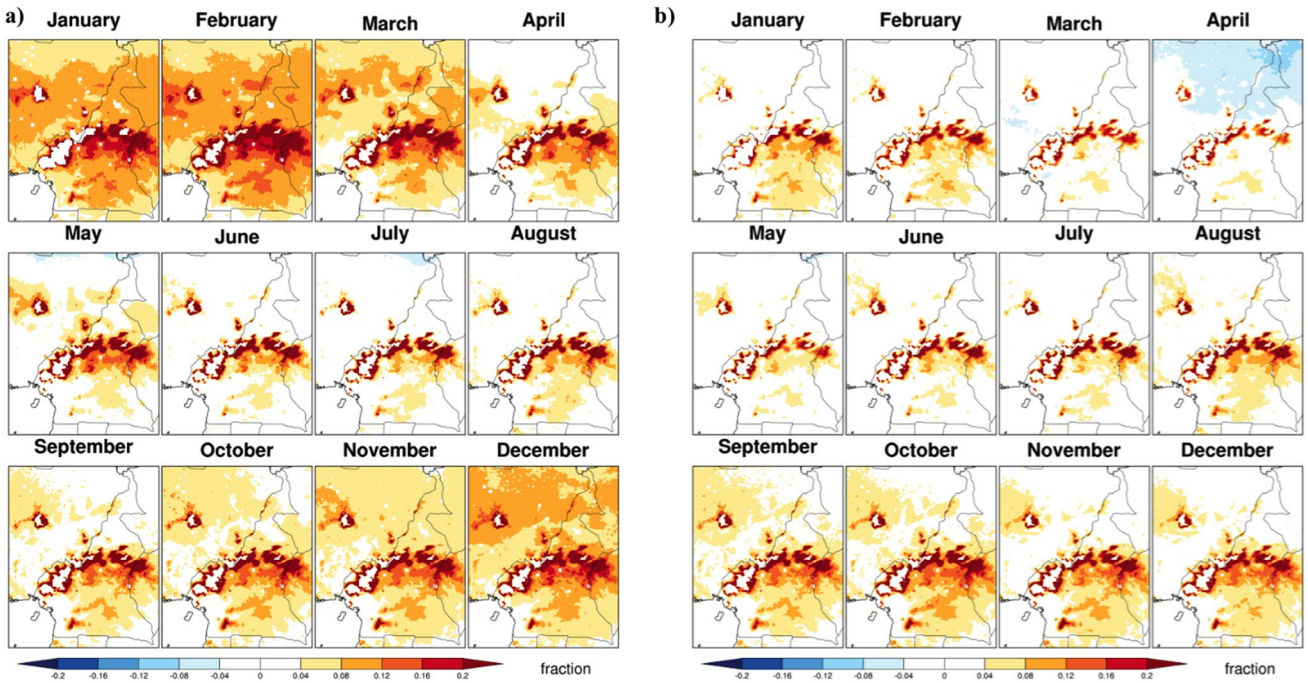

Fig. 6 Monthly mean changes in PR under RCP2.6 scenario. VECTRI model driven by RCA4-EnsMean for the period 2035–2065 (**a**) and 2071–2100 (**b**)

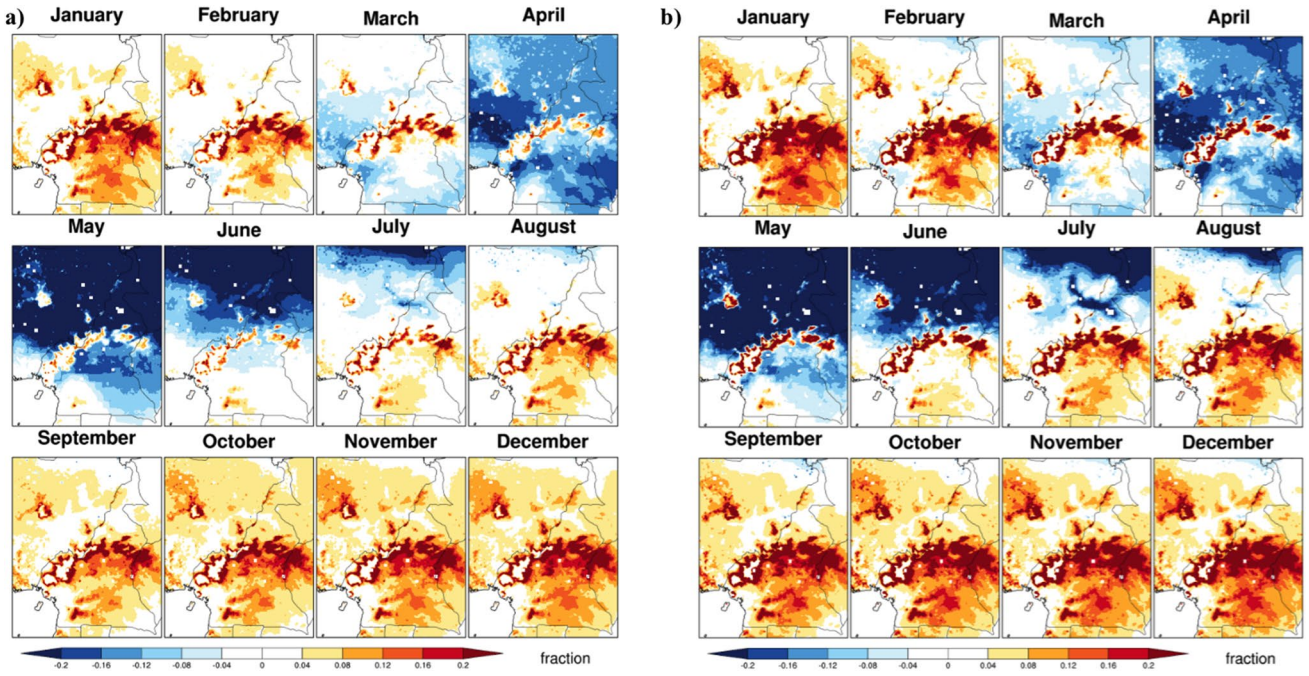

Fig. 7 Monthly mean changes in PR under RCP8.5 scenario. VECTRI model driven by RCA4-EnsMean for 2035–2065 (**a**) and 2071–2100 (**b**)

The PR tends to decrease when VECTRI is forced with RCA4-EC-EARTH-ES (Fig. S1) experiment with respect to other VECTRI-RCA4 runs. Contrastingly, increases instead are expected in the PR when VECTRI is driven by RCA4-HadGEM2 (Fig. S7).

PR is then projected to increase throughout the year with emphasis from October to March over the near future (Fig. 6a). A similar pattern is observed over the far future (Fig. 6b), where the PR tends to mostly increase over WCAM and decreases during the April month in NCAM. The PR is projected to significantly decrease in the distant future than in the near future.

Figure 7 presents the PR pattern with RCA-EnsMean as forcing under RCP8.5 scenario. Results based on individual forcings of VECTRI by RCA4 experiments are highlighted in the supplementary material: Fig. S2 for RCA4-EC-EARTH-ES, Fig. S4 for RCA4-MPI-ESM-LR, Fig. S6 for RCA4-MIROC5, Fig. S8 for RCA4-HadGEM2 and Fig. S10 for RCA4-NorESM1-M. The increase in the PR is strongest when VECTRI is coupled with RCA4-HadGEM2 (Fig. S8).

Under the high emission scenario RCP8.5 (Fig. 7), obvious differences between the near (Fig. 7a) and the far (Fig. 7b) future appear in the amplitude of changes in the PR. The PR generally tends to decrease from March to July, especially over NCAM, and increase during the rest of the year, especially over WCAM and ECAM.

The above results indicate that global warming would not much change the life cycles of the Anopheles mosquito and the malaria parasite *plasmodium falciparum.* Actually, rainfall creates suitable conditions (availability of ponds) for the mosquitoes' breeding process. But extreme rainfall could negatively impact the productivity of mosquito breeding habitat by flushing effect which leads to high mosquito losses (Paaijmans et al. 2010). This is observed in Figs. 6 and 7 from April to September referring to rainfall patterns in Figs. S21 and S23 of the Supplementary material.

Moreover, PR tends to intensify with temperature values less than 32 °C (see Figs. S22 and S24 in the supplementary material). This is associated with the fact that there is a range of temperatures that allows malaria transmission. In fact, the temperature is able to create good conditions for malaria vectors to thrive. Generally, the increase in temperature accelerates vector life cycles and also decreases the incubation period of the parasite (Van-Lieshout et al. 2004). This result is in line with previous studies conducted over Cameroon. They showed that the temperature suitability range for *Anopheles gambiae* and *Anopheles funestus* is between 20 and 29 °C (Tanga et al. 2010). Similar results were reported over the Limpopo Province in South Africa (Komen et al. 2015). However, at a very high temperature, mortality is high thus reducing transmission (Ebi et al. 2005), which corresponds to the situation expected in NCAM (Fig. 7 from April to July) and previously reported by Chemison et al. (2021) and Caminade et al. (2014).

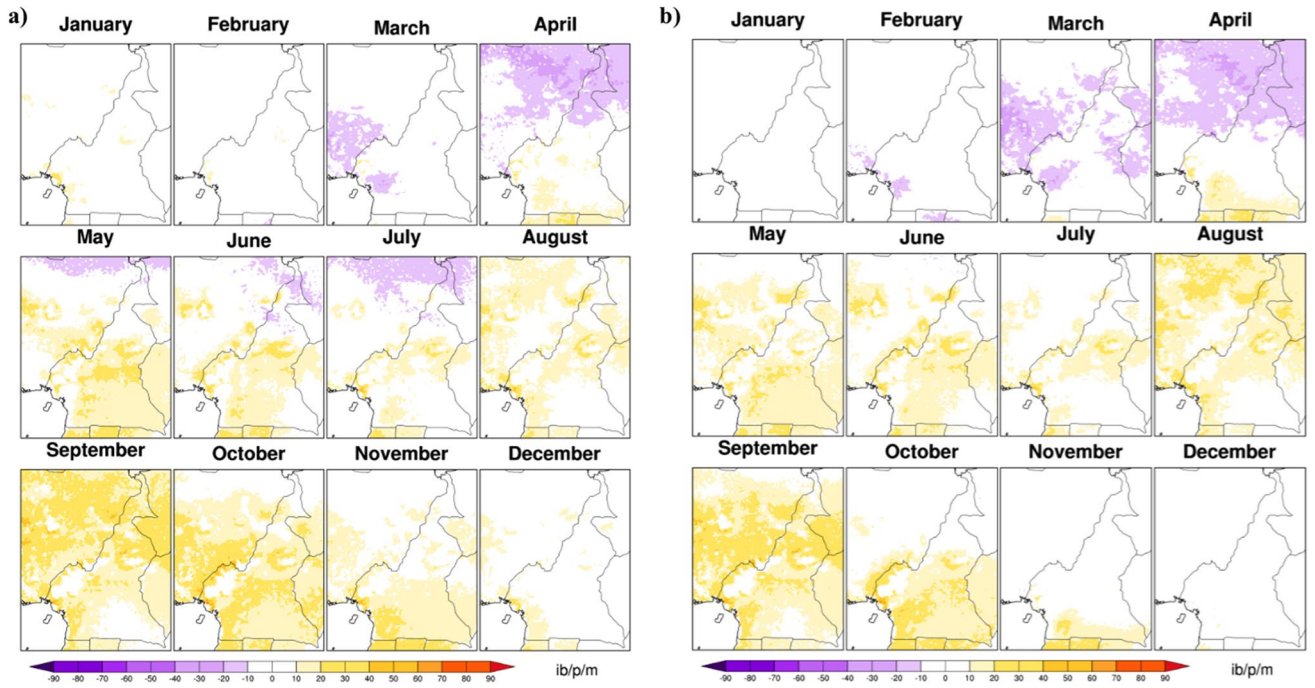

Fig. 8 Monthly estimated changes in EIR indicating the number of infected bites per person per month (ib/p/m). This is obtained for the RCP2.6 scenario from the coupling VECTRI-RCA4-EnsMean over the periods 2035–2065 (**a**) and 2071–2100 (**b**)

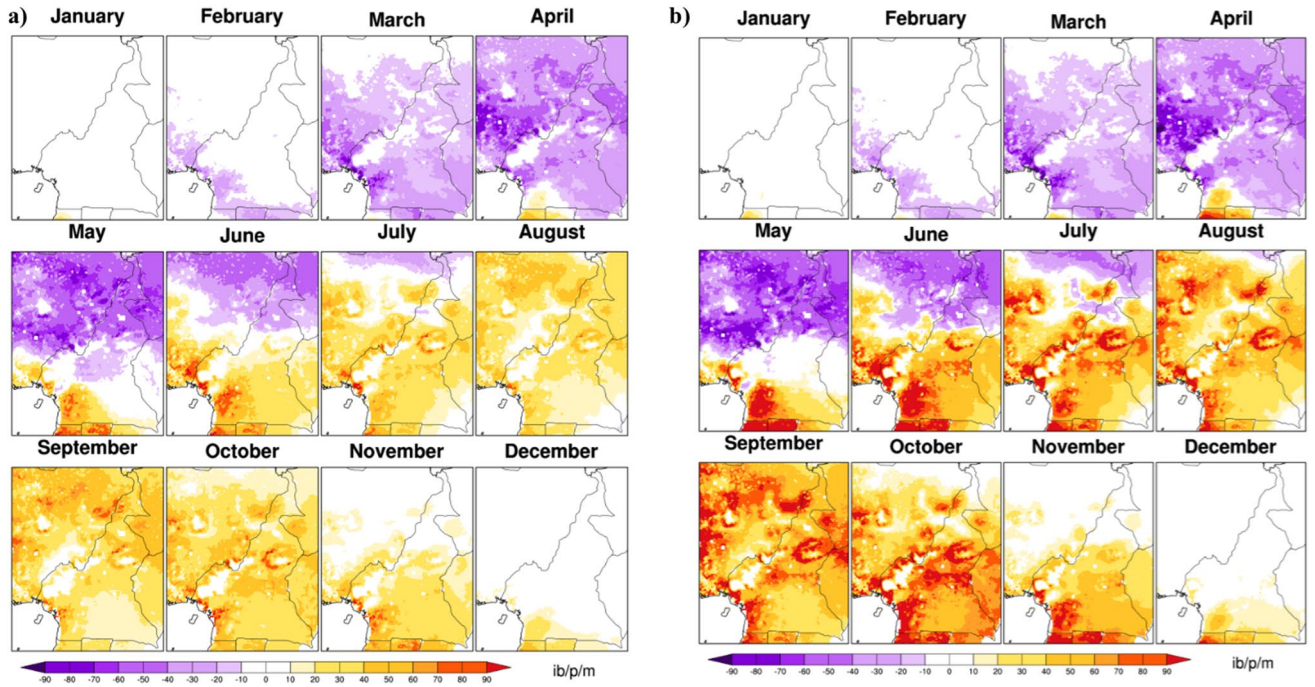

Fig. 9 Monthly estimated changes in EIR, indicating the number of infected bites per person per month (ib/p/m). Results obtained from the coupling VECTRI-RCA-EnsMean under the RCP8.5 scenario and over 2035–2065 (**a**) and 2071–2100 (**b**) periods

Changes in the entomological inoculation rate (EIR)

Figures 8 and 9 display maps of monthly mean changes in the EIR pattern when VECTRI is forced by RCA4-EnsMean under RCP2.6 and RCP8.5 respectively.

Broadly under RCP2.6, EIR is projected to decrease from April to July in NCAM and during March in WCAM (Fig. 8a). In the distant future, the EIR is expected to reduce from March to April, especially over NCAM (Fig. 8b). Over WCAM and ECAM subregions, an intensification of EIR is projected from April to November, whereas insignificant changes will occur for December and January.

For individual RCA4 model simulations, results are shown in the supplementary materials (Figs. S11, S13, S15, S17 and S19). EIR tends to gradually increase when VECTRI is forced with RCA4-HadGEM2 (Fig. S17), from June (WCAM and ECAM) to November with a peak in August to September (NCAM). There is a decrease in projections using rainfall and temperature from RCA4-EC-EARTH-ES (Fig. S11), whereas fewer changes are expected in EIR with RCA4-NorESM1-M (Fig. S19).

Under RCP8.5, EIR is expected to decrease significantly over almost the entire study area during March and April months and especially over NCAM from May to June (Fig. 9a and b). Conversely, EIR is projected to increase over WCAM and ECAM from May to November and over NCAM from July to November. No particular changes are foreseen over almost the whole country from December to February, except for a small part of southern Cameroon where a strengthening of the EIR is noted in December and a weakening in February over the two projection periods.

Results with the coupling VECTRI-RCA4-EC-EARTH-ES, VECTRI-RCA4-MPI-ESM-LR, VECTRI-RCA4-MIROC5, VECTRI-RCA4-HadGEM2 and VECTRI-RCA4-NorESM1-M are presented in Figs. S12, S14, S16, S18 and S19, respectively.

Changes in EIR presented in Figs. 8 and 9 can be explained by the suitable range of temperature of 18–33 °C (Bayoh and Lindsay 2003) of the study area as highlighted in Figs. S22 and S24 in the supplementary material. But it should be recalled that temperatures above 30 °C are prejudicial for anopheles' development, therefore leading to a decrease in EIR as demonstrated in Béguin et al. (2011).

Changes in EIR are stronger in the far future than in the near future and vice-versa (Figs. 8 and 9). In general, the signal of change is stronger under RCP8.5 than RCP2.6, meaning an increased risk with the increased level of the radiative forcing. A similar study conducted by Chaturvedi and Dwivedi (2021) over India showed that under global warming, malaria transmission is expected to strengthen together with the duration of the transmission season. The EIR results also highlight the important role of changes in rainfall and temperature on malaria incidence and show the seasonality of the disease. Similar work also demonstrated that a decline in precipitation is beneficial for the growth of the mosquito population, which causes higher EIR (Ermert et al. 2012). Our study also attests to general expectations with regard to the impact of global warming on the spread of malaria. It is generally accepted that climate change will affect the spread of malaria as mentioned by Ogega and Alobo (2020), but it is also noted that malaria distribution is impacted by many factors in addition to climate change, including population mobility, changes in land use, changes in air and water temperatures and the systematic increase in preventive interventions, which VECTRI has not yet incorporated and which should prompt future work.

Conclusion

This work is an initial exploration of the relationship between climate and malaria in Cameroon using dynamical models under future climate scenarios of the CORDEX project for Africa. The link between these parameters and two common malaria indicators, parasite ratio (PR) and entomological inoculation rate (EIR), was established. The results demonstrated that there is a close relationship between rainfall, temperature and malaria transmission in Cameroon under future climate change. For each of the models used under the two RCP scenarios, the impact of temperature on the evolution of malaria indicators is established, and the seasonality is highlighted for the PR and EIR metrics. The integration of VECTRI with future climate scenarios reveals a modulating effect of changes in temperature and rainfall on changes in malaria transmission, although factors such as population mobility and effective intervention strategies against malaria are likely to improve VECTRI results if implemented. The next step in line of this work is to ascertain how best to incorporate such a model effectively into a national or regional decision-making process concerning health planning and interventions. If such a model should be used to aid operational decisions in Cameroon, using machine learning techniques for an effectiveness model's calibration of parameters is required as recently introduced in Tompkins and Thomson (2018).

Supplementary Information The online version contains supplementary material available at https://doi.org/10.1007/s00484-022-02388-x.

Acknowledgements The authors acknowledge Dr Adrian Mark Tompkins for providing the VECTRI model and supporting information. The second author also acknowledges the support from the DAAD within the framework of the ClimapAfrica programme. The authors also thank members of the LEMAP laboratory at the University of Yaounde I for their support. The authors would like to acknowledge the Rossby Centre, Swedish Meteorological and Hydrological Institute (SMHI), Norrköping, Sweden, where RCA4 simulations are performed. We also acknowledge all the reanalysis and observational data providers used

in this study. We are grateful to anonymous reviewers and the editor for the thorough reviews and critical comments.

Data availability RCA4 output data are available through the Earth System Grid Federation (ESGF) website (https://esgf-data.dkrz.de/search/cordex-dkrz/). The ERA-Interim reanalysis is available from the European Centre for Medium-Range Weather Forecast (ECMWF) and can be downloaded through the link: https://apps.ecmwf.int/datasets/data/interim-full-daily/levtype=sfc/. The CHIRPS2 data are available at https://data.chc.ucsb.edu/products/CHIRPS-2.0/global_daily/netcdf/.

Declarations

Competing interests The authors declare no competing interests.

References

Abiodun GJ, Witbooi P, Okosun KO (2018) Modelling the impact of climatic variables on malaria transmission. Hacettepe J. Math Stat 47:219–235. https://doi.org/10.15672/HJMS.2017.452

Asare EO, Amekudzi LK (2017) Assessing climate driven malaria variability in Ghana using a regional scale dynamical model. Climate 5(1):20. https://doi.org/10.3390/cli5010020

Ayanlade A, Sergi C, Ayanlade OS (2020) (2020) Malaria and meningitis under climate change: initial assessment of climate information service in Nigeria. Meteorol Appl 27:e1953. https://doi.org/10.1002/met.1953

Bandolo FMN (2012) Heavily indebted poor countries (HIPC) initiative in cameroon and the fight to reduce malaria related under-five mortality (Master's thesis, Høgskolen i Oslo og Akershus. Fakultet for samfunnsfag). https://hdl.handle.net/10642/1803

Bayoh MN, Lindsay SW (2003) Effect of temperature on the development of the aquatic stages of Anopheles gambiae sensu stricto (Diptera: Culicidae). Bull Entomol Res 93(5):375–381. https://doi.org/10.1079/BER2003259

Béguin A, Hales S, Rocklöv J, Åström C, Louis VR, Sauerborn R (2011) The opposing effects of climate change and socio-economic development on the global distribution of malaria. Glob Environ Chang 21(4):1209–1214. https://doi.org/10.1079/BER2003259

Bentsen M, Bethke I, Debernard J, Iversen T, Kirkevåg A, Seland Ø, Drange H, Roelandt C, Seierstad I, Hoose C et al (2013) The Norwegian earth system model, NORESM1-part 1: description and basic evaluation of the physical climate. Geosci Model Dev 6(3):687–720. https://doi.org/10.5194/gmd-6-687-2013

Bomblies A, Eltahir EA (2009) Assessment of the impact of climate shifts on malaria transmission in the Sahel. EcoHealth 6(3):426–437. https://doi.org/10.0007/s10393-010-0274-5

Caminade C, Kovats S, Rocklov J, Tompkins AM, Morse AP, Colón-González FJ, Lloyd SJ (2014) Impact of climate change on global malaria distribution. Proc Natl Acad Sci. https://doi.org/10.1073/pnas.130289111

Chaturvedi, Dwivedi S (2021) Understanding the effect of climate change in the distribution and intensity of malaria transmission over India using a dynamical malaria model. Int J Biometeorology 1-15.https://doi.org/10.1007/s00484-021-02097-x

Chemison A, Ramstein G, Tompkins AM, Defrance D, Camus G, Charra M, Caminade C (2021) Impact of an accelerated melting of Greenland on malaria distribution over Africa. Nat Commun 12(1):1–12. https://doi.org/10.1038/s41467-021-24134-4

Collins WJ, Bellouin N, Doutriaux-Boucher M, Gedney N, Halloran P, Hinton T, Hughes J, Jones CD, Joshi M, Liddicoat S, Martin G, O'Connor F, Rae J, Senior C, Sitch S, Totterdell I, Wiltshire A, Woodward S (2011) Development and evaluation of an earth-system model HadGEM2. Geosci Model Dev 4(4):1051–1075.https://doi.org/10.5194/gmd-4-1051-2011 https://www.geosci-model-dev.net/4/1051/2011/

Costello A, Abbas M, Allen A, Ball S, Bell S, Bellamy R, Friel S, Groce N, Johnson A, Kett M, Lee M (2009) Managing the health effects of climate change: lancet and University College London Institute for Global Health Commission. The Lancet 373(9676):1693–1733

Day KP, Hayward RE, Dyer M (1998) The biology of Plasmodium falciparum transmission stages. Parasitology-Cambridge 116:S95–S110

Dee DP, Uppala SM, Simmons AJ, Berrisford P, Poli P, Kobayashi S, Andrae U, Balmaseda MA, Balsamo G, Bauer DP, Bechtold P (2011) The ERA-Interim reanalysis: Configuration and performance of the data assimilation system. Q J R Meteorol Soc 137(656):553–597. https://doi.org/10.1002/qj.828

Diouf I, Rodriguez-Fonseca B, Deme A, Caminade C, Morse AP, Cisse M, Gaye AT (2017) Comparison of malaria simulations driven by meteorological observations and reanalysis products in Senegal. Int J Environ Res Public Health 14(10):1119. https://doi.org/10.3390/ijerph14101119

Diouf I, Fonseca BR, Caminade C, Thiaw WM, Deme A, Morse AP, Ndione JA, Gaye AT, Diaw A, Ndiaye MKN (2020) Climate variability and malaria over West Africa. Am J Trop Med Hyg 102(5):1037. https://doi.org/10.4269/ajtmh.19-0062

Ebi KL, Hartman J, Chan N, Mcconnell J, Schlesinger M, Weyant J (2005) Climate suitability for stable malaria transmission in Zimbabwe under different climate change scenarios. Clim Change 73(3):375–393. https://doi.org/10.1007/s10584-005-6875-2

Egbendewe-Mondzozo A, Musumba M, McCarl BA, Wu X (2011) Climate change and vector-borne diseases: an economic impact analysis of malaria in Africa. Int J Environ Res Public Health 8(3):913–930. https://doi.org/10.3390/ijerph8030913

Ermert V, Fink AH, Morse AP, Paeth H (2012) The impact of regional climate change on malaria risk due to greenhouse forcing and land-use changes in tropical Africa. Environ Health Perspect 120(1):77–84. https://doi.org/10.1289/ehp.1103681

Escobar LE, Romero-Alvarez D, Leon R, Lepe-Lopez MA, Craft ME, Borbor-Cordova MJ, Svenning JC (2016) Declining prevalence of disease vectors under climate change. Sci Rep 6(1):1–8. https://doi.org/10.1038/srep39150

Garske Tini, Ferguson Neil M, Ghani Azra C (2013) Estimating air temperature and its influence on malaria transmission across Africa. PloS one 8(2):e56487. https://doi.org/10.1371/journal.pone.0056487

Hajison PL, Mwakikunga BW, Mathanga DP, Feresu SA (2017) Seasonal variation of malaria cases in children aged less than 5 years old following weather change in Zomba district, Malawi. Malaria J 16(1):1–12. https://doi.org/10.1186/s129336-017-1913-x

Hazeleger W, Severijns C, Semmler T, Ştefănescu S, Yang S, Wang X, ... Willén U (2010) EC-Earth: a seamless earth-system prediction approach in action. Bull Am Meteorol Soc 91(10):1357-1364.https://doi.org/10.1175/2010BAMS2877.1

Komen K, Olwoch J, Rautenbach H, Botai J, Adebayo A (2015) Long-run relative importance of temperature as the main driver to malaria transmission in Limpopo Province, South Africa: a simple econometric approach. EcoHealth 12(1):131–143. https://doi.org/10.1007/s10393-014-0992-1

Linard C, Gilbert M, Snow RW, Noor AM, Tatem AJ (2012) Population distribution, settlement patterns and accessibility across Africa in 2010. PLoS One 7(2):e31743. https://doi.org/10.1371/journal.pone.0031743

Lindsay SW, Bødker R, Malima R, Msangeni HA, Kisinza W (2000) Effect of 1997–98 EI Niño on highland malaria in Tanzania.

The Lancet 355(9208):989–990. https://doi.org/10.1016/S0140-6736(00)90022-9
Love T (2022) The climate prediction center rainfall algorithm version 2." NOAA Climate Prediction Center Tech. http://www.cpc.ncep.noaa.gov/products/fews/RFE2.0_tech.pdf. Accessed May 2022
Mbarga B (2010) 3eme rgph. rapport de présentation des résultats définitifs. BUCREP (Bureau Central des Recensements et des Etudes de la Population), Yaoundé. http://www.bucrep.cm/index.php/fr/component/phocadownload/category/20-prsentation-des-rsultats
Mbouna AD, Tompkins AM, Lenouo A, Asare EO, Yamba EI, Tchawoua C (2019) (2019) Modelled and observed mean and seasonal relationships between climate, population density and malaria indicators in Cameroon. Malar J 18(1):359. https://doi.org/10.1186/s112936-019-2991-8
Molua EL, Lambi CM (2007) The economic impact of climate change on agriculture in cameroon, Volume 1of 1. The World Bank.
Ngarakana-Gwasira ET, Bhunu CP, Masocha M, Mashonjowa E (2016) Assessing the role of climate change in malaria transmission in Africa. Malaria Res Treat 2016.https://doi.org/10.1155/2016/7104291
Ogega OM, Alobo M (2020) Impact of 1.5 o C and 2 o C global warming scenarios on malaria transmission in East Africa [version 2; peer review. https://doi.org/10.12688/aas0penres.13074.1
Paaijmans KP, Wandago MO, Githeko AK, Takken W, Carter D (2007) Unexpected high losses of anopheles gambiae larvae due to rainfall. PLoS ONE 2(11):e1146. https://doi.org/10.1371/journal.pone0001146
Paaijmans KP, Blanford S, Bell AS, Blanford JI, Read AF, Thomas MB (2010) Influence of climate on malaria transmission depends on daily temperature variation. Proc Natl Acad Sci 107(34):15135–15139. https://doi.org/10.1073/pnas.1006422107
Peterson AT (2009) Shifting suitability for malaria vectors across Africa with warming climates. BMC Infect Dis 9(1):1–6. https://doi.org/10.1186/147-2334-9-59
Popke Dagmar, Stevens Bjoern, Voigt Aiko (2013) Climate and climate change in a radiative-convective equilibrium version of ECHAM6. J Adv Model Earth Syt 5(1):1–14. https://doi.org/10.1029/2012MS000191
Tanga MC, Ngundu WI, Judith N, Mbuh J, Tendongfor N, Simard F, Wanji S (2010) Climate change and altitudinal structuring of malaria vectors in south-western Cameroon: their relation to malaria transmission. Trans R Soc Trop Med Hyg 104(7):453–460. https://doi.org/10.1016/j.trstmh.2010.02.006
Taylor KE, Stouffer RJ, Meehl GA (2012) An overview of CMIP5 and the experiment design. Bull Am Meteor Soc 93(4):485–498. https://doi.org/10.1175/bams-d-11-00094.1
Tompkins AM, Ermert V (2013) A regional-scale, high resolution dynamical malaria model that accounts for population density, climate and surface hydrology. Malar J 12(1):65. https://doi.org/10.1186/1475-2875-12-65
Tompkins AM, Thomson MC (2018) Uncertainty in malaria simulations in the highlands of Kenya: relative contributions of model parameter setting, driving climate and initial condition errors. PLoS ONE 13(9):e0200638. https://doi.org/10.1371/journal.pone.0200638
Van Lieshout M, Kovats RS, Livermore MTJ, Martens P (2004) Climate change and malaria: analysis of the SRES climate and socio-economic scenarios. Glob Environ Change 14(1):87–99. https://doi.org/10.1016/j.gloenvcha.2003.10.009
Watanabe S, Hajima T, Sudo K, Nagashima T, Takemura T, Okajima H, Nozawa T, Kawase H, Abe M, Yokohata T et al (2011) Miroc-esm 2010: model description and basic results of cmip5- 20c3m experiments. Geosci Model Dev Discuss 4:1063–1128. https://doi.org/10.5194/gmdd-4-1063-2011
World Health Organization, World malaria report (2008) Geneva: WHO library cataloguing-in-publication data. p 215. https://www.who.int/publications/i/item/9789241563697
World Health Organization and Mahler, Halfdan (1975) The work of WHO, 1974: annual report of the Director-General to the World Health Assembly and to the United Nations. World Health Organization. https://apps.who.int/iris/handle/10665/85882. Accessed May 2022
World Health Organization (2015) World malaria report 2015. World Health Organization. https://apps.who.int/iris/handle/10665/200018. Accessed May 2022
Yamana TK, Bomblies A, Eltahir EA (2016) Climate change unlikely to increase malaria burden in West Africa. Nat Clim Chang 6(11):1009–1013. https://doi.org/10.1038/nclimate3085
Yamba EI, Tompkins AM, Fink AH, Ermert V, Amelie MD, Amekudzi LK, Briët OJT (2020) Monthly Entomological Rate Data for Studying the Seasonality of Malaria Transmission in Africa. Data 5(2):31. https://doi.org/10.3390/data5020031
Yé Y, Louis VR, Simboro S, Sauerborn R (2007) Effect of meteorological factors on clinical malaria risk among children: an assessment using village-based meteorological stations and community-based parasitological survey. BMC public health 7(1):1–11. https://doi.org/10.1186/1471-2458-7-101
Zaroug MG, Reynolds S (2006) Country pasture/forage resource profiles. FAO, Rome